Belhocine reviews recent reports on the role of ^{18}F-FDG PET imaging as a reliable means of monitoring after therapy for cervical cancer. ..... ***Page 1602***

Schäfers and colleagues use gated SPECT to assess functional remodeling after partial left ventriculectomy in patients with dilated cardiomyopathy. ..... ***Page 1605***

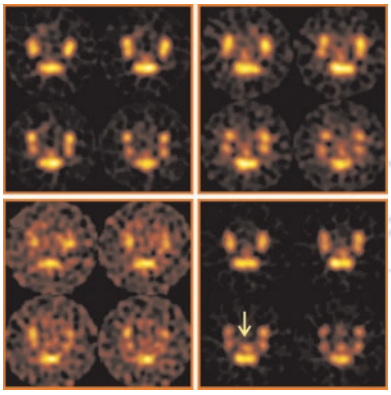

Graf and colleagues compare nonfluoroscopic electroanatomic mapping with SPECT perfusion and PET metabolic imaging in the assessment of myocardial viability in patients with coronary artery disease. ..... ***Page 1611***

Fricke and colleagues report on a method to improve coregistration and reduce artifacts resulting from miasalignment in attenuation-corrected myocardial perfusion SPECT. ..... ***Page 1619***

Koepfli and colleagues use PET to explore the effects of long-term β-receptor blocker treatment on myocardial blood flow and coronary vasodilatory capacity in patients with coronary artery disease. ..... ***Page 1626***

Lai and colleagues devise a prognostic scoring system based on clinical, treatment, and laboratory factors to indicate which patients could benefit most from ^{18}F-FDG PET restaging for salvage therapy in recurrent cervical cancer. ..... ***Page 1632***

Keidar and colleagues compare ^{18}F-FDG PET/CT with side-by-side PET and CT in suspected recurrent lung cancer and evaluate the relative effects on patient management. ..... ***Page 1640***

Signore and colleagues report on ^{99m}Tc-interleukin 2 scintigraphy as a means of measuring tumor infiltration to identify patients with suspected melanoma who may benefit from immunotherapy. ..... ***Page 1647***

Spence and colleagues look at possible diagnostic benefits in delaying the interval between ^{18}F-FDG administration and PET data acquisition in imaging gliomas. ..... ***Page 1653***

Nguyen and colleagues assess the long-term benefits of radionuclide therapy with ^{111}In-pentetreotide and ^{131}I-MIBG in patients with advanced-stage gastroenteropancreatic neuroendocrine tumors uncontrolled by other therapies. .. ***Page 1660***

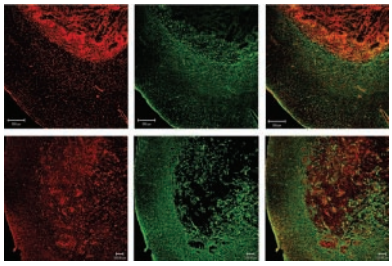

Shu-Hang and colleagues evaluate the sensitivity and specificity of ^{18}F-FDG PET in detection of recurrent nasopharyngeal carcinoma in patients after questionable MRI findings. ..... ***Page 1669***

Cobben and colleagues investigate the utility of ^{18}F-FLT PET in staging and restaging of disease in patients with non–small cell lung cancer. ..... ***Page 1677***

Schechter and colleagues report on the dosimetric properties of ^{99m}Tc-ethylene dicysteine C225 as a novel diagnostic agent in squamous cell carcinoma of the head and neck and as a possible screening agent to select candidates for C225 therapy. ..... ***Page 1683***

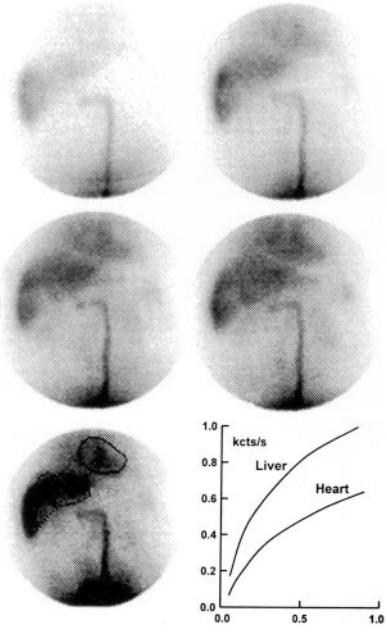

Lorberboym and colleagues assess functional imaging with ^{123}I-FP-CIT in patients with cerebrovascular disease to identify those who will most benefit from treatment for vascular parkinsonism. ..... ***Page 1688***

Schwarz and colleagues provide data on the decline in dopamine transporter binding in Parkinson's disease and present evidence for a new model of disease progression. ..... ***Page 1694***

Bennink and colleagues report on the use of ^{99m}Tc-HMPAO white blood cell scintigraphy as a reliable, noninvasive tool both in predicting therapeutic re-

sponse and in follow-ups of patients with ulcerative colitis. . . . . ***Page 1698***

Vajro and colleagues assess the clinical utility of ^{99m}Tc-pertechnetate per-rectal portal scintigraphy as a minimally invasive tool for better assessment and follow-up of portal hypertension in children with chronic cholestasis. . . . ***Page 1705***

Krausz and colleagues report changes in regional cerebral blood flow in patients both before and after treatment for mild hypothyroidism. . . . . ***Page 1712***

Capello and colleagues investigate the increased therapeutic potential of linking RGD peptides to somatostatin analogs and discuss possible clinical applications. . . . . ***Page 1716***

Meine and colleagues review the role of nuclear medicine in the combined assessment of myocardial perfusion and left ventricular function, including the ability of new modalities to enhance the diagnosis and prognosis of coronary artery disease. . . . . ***Page 1721***

Wessels and colleagues analyze reported marrow dosimetry results from radioimmunotherapy trials and propose a standard, benchmark method for marrow dosimetry for radiolabeled antibodies. . . . . ***Page 1725***

Mawlawi and colleagues describe the 2- and 3D performance characteristics and whole-body imaging suitability of a newly developed PET/CT scanner using the National Electrical Manufacturers Association NU94 and NU01 standards. . . . . ***Page 1734***

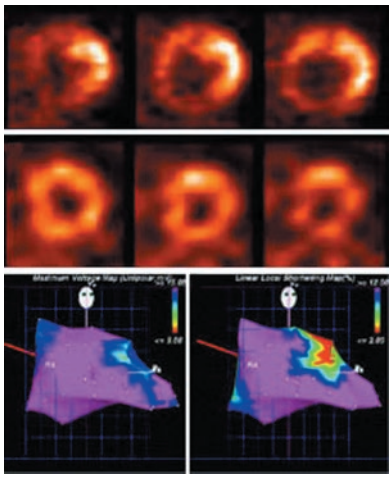

Anton and colleagues report on an in vitro demonstration of the usefulness of a vector coexpressing HSV1-tk and VEGF for noninvasive imaging of expression of a therapeutic transgene. . . . ***Page 1743***

Eerd and colleagues test the imaging characteristics of ^{111}In-labeled LTB4 antagonist DPC11870 in New Zealand White rabbits with experimental pulmonary aspergillosis infection. . ***Page 1747***

Sugiyama and colleagues report on investigations in a mouse model on the feasibility of ^{18}F-FLT as a PET tracer for imaging tumor proliferation and monitoring response to therapy. . . . ***Page 1754***

van Montfrans and colleagues evaluate a scintigraphic technique to assess lymphocyte homing to the colon in experimental colitis in a rat model. . ***Page 1759***

Suzuki and colleagues image endogenous gene expression in brain cancer using peptide nucleic acid antisense agents modified to enable crossing of biologic membrane barriers and access to intracellular target mRNA molecules. . . . . ***Page 1766***

Chen and colleagues introduce and evaluate an improved peptide tracer for microPET imaging in brain tumor models and outline its potential applications in both imaging and therapy. . . ***Page 1776***

Schaffland and colleagues research ^{131}I-labeling of rituximab using 2 different radioiodination degrees as part of a search for optimal conditions for radioimmunotherapy of lymphoma. . . . . ***Page 1784***

ON THE COVER

This patient was judged as showing positive findings on ^{99m}Tc-scintigraphy. Despite the small size of the tumor (green arrow), regional lymph nodes are detectable (red arrow), reflecting an active immune response inside the primary and metastatic tumors. The target-to-background radioactivity ratio is 1.44. CD25 staining shows a mild positivity for neoplastic cells and a strong, diffuse positivity for lymphocytes.